SAE TECHNICAL
PAPER SERIES

930814

Formability of Type 304 Stainless Steel Sheet

G. J. Coubrough
EG & G

D. K. Matlock and C. J. Van Tyne
Colorado School of Mines

Reprinted from:
Sheet Metal and Stamping Symposium
(SP-944)

The Engineering Society
For Advancing Mobility
Land Sea Air and Space®
INTERNATIONAL

International Congress and Exposition
Detroit, Michigan
March 1-5, 1993

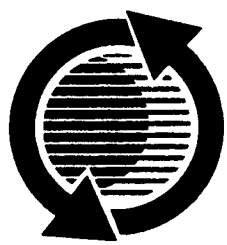

ISSN 0148-7191

Printed in USA

930814

Formability of Type 304 Stainless Steel Sheet

G. J. Coubrough
EG & G

D. K. Matlock and C. J. Van Tyne
Colorado School of Mines

ABSTRACT

Punch-stretch tests to determine formability of type 304 stainless steel sheet were conducted using a hemispherical dome test. Sheets of 19.1 mm width and 177.8 mm width were stretched on a 101.6 mm diameter punch at punch rates between 0.042 to 2.12 mm/sec with three lubricant systems: a mineral seal oil, thin polytetrafluoroethelyne sheet with mineral seal oil, and silicone rubber with mineral seal oil. The resulting strain distributions were measured and the amount of martensite was determined by magnetic means. Increasing lubricity resulted in more uniform strain distributions while increased punch rates tended to decrease both strain and transformation distributions. High forming limit values were related to the formation of high and uniformly distributed martensite volume fractions during deformation. The results of this study are interpreted with an analysis of the effects of strain and temperature on strain induced martensite formation in metastable austenitic stainless steels.

INTRODUCTION

Sheet metal forming operations often employ stretching as a primary deformation mode. Stretching limits depend primarily on the uniformity of the strain distribution and acceptable strain limits which are represented by a forming limit curve (FLC). An FLC shows the onset of localized necking for all strain combinations that may exist in the plane of a sheet and can be derived from data obtained in a hemispherical punch test [1]. In hemispherical punch tests, the imposed strain state varies with specimen width: narrow specimens produce a uniaxial stress state resulting in a tensile and compressive surface strain, while fully constrained sheets produce a biaxial stress state causing both surface strains to be tensile.

Strain uniformity in forming operations is controlled by both extrinsic and intrinsic factors. Extrinsic factors are production related and include the punch rate, lubrication and part geometry. Intrinsic factors relate to material properties of the sheet. Production requirements often result in material properties being pushed to the limit. Detailed studies of strain distribution during punch stretching have been reported by Keeler [2], Heyer [3], and Hecker [4]. The majority of the studies to date have considered ferritic steels and aluminum alloys. However, with the increased use of stainless steel sheet products in automotive applications, a complete understanding of the formability of austenitic and ferritic stainless steels is required in order to optimize properties. The investigation considered in this paper examines the interrelation between strain distribution and microstructure of type 304 stainless steel sheet punch stretched over a hemispherical dome. Previous studies on this material have been conducted under uniaxial tension [5-8].

Deformation of 304 stainless steel results in the strain-induced transformation of fcc austenite (γ) to bcc martensite (α') at temperatures below M_d, the deformation assisted martensite start temperature [7]. The effects of strain and temperature on strain-induced transformation in type 304 stainless steel have been modeled by Olson and Cohen [9], and their predictions correlate with sigmoidal-shaped curves of volume fraction martensite as a function of strain as shown in Figure 1 [5,10].

Isothermal tensile testing has shown that the extent of transformation affects mechanical properties [8]. Huang et al [8] considered total strains as the sum of the uniform strain and the post-uniform strain and found that with an increase in temperature, the uniform strain, post-uniform strain and the total strains all exhibited maxima. However, the temperatures at which the maximum values occurred were not the same. More specifically, it was found that at low temperatures, transformation is essentially complete prior to necking. As temperature increases, the strain required to complete transformation also increases. At temperatures above 0°C, the strain-induced martensite transformation is deferred to strains greater than the maximum uniform elongation. At the onset of necking, local strains and strain rates increase within the neck and significant

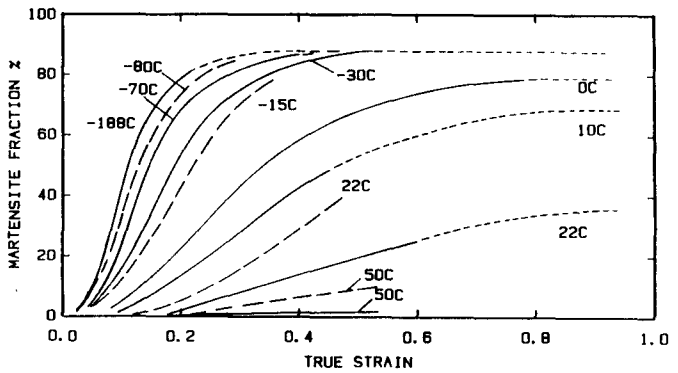

Figure 1. Volume fraction of martensite (α') formed during uniaxial tension as a function of true strain at different temperatures. Solid lines are data of Angel [5], dots are Olson-Cohen extrapolation [9], and dashed lines are Hecker et al. [10].

dynamic strengthening due to the martensite transformation results. Martensite formation within the neck stabilizes local flow to produce a maximum in the post-uniform strain at temperatures between 25°C to 90°C. At high temperatures, above the M_d temperature, austenite is stable at all strains. Not only is there no strengthening due to martensite formation in the uniform elongation stage, but the potential for dynamic strengthening in the necked region is low and a decrease in the post-uniform strain occurs.

For this investigation, 304 stainless steel sheets were stretched on a hemispherical dome test system at various punch rates. Strain distributions were altered by changing sheet width and lubrication conditions. The resulting strain distributions were measured and the amount of martensite was determined by magnetic means. The role of lubrication and punch rate as related to the martensite transformation and their combined effects on formability are discussed.

EXPERIMENTAL PROCEDURE

Punch stretch tests were conducted on a hemispherical dome test system which conforms to the standard limiting dome height (LDH) test geometry and which was adapted to a commercial floor model servo-hydraulic test system [11]. Sheet specimens, clamped between two die platens, were stretched to failure over a 101.6 mm (4 in.) diameter spherical steel punch. Test execution and data acquisition were controlled by a personal computer system; tests were performed in stroke control at punch rates between 0.042 and 2.12 mm/sec while punch force, height and thermocouple data were collected. All samples were deformed until localized necking or fracture occurred with the concurrent maximum punch height recorded as the LDH value.

Three lubrication conditions were used and are listed in order of increasing lubricity: a) a mineral seal oil, (referred to as 'oil'); b) polytetrafluoroethelyne sheet (0.5 mm thick) with mineral seal oil ('PTFE'); and c) RTV silicone rubber sheet (12.7 mm thick) with mineral seal oil ('RTV'). The presence of the RTV rubber disk altered the strain distribution to produce a condition similar to that obtained in a hydraulic bulge test, except that the final dome shape was modified due to the fact that the effective punch diameter was greater with the rubber sheet in place.

Specimens were sheared from 0.864 mm (0.034 in.) gauge sheet. The rolling direction was maintained along the length of the specimen. Two specimen configurations were used in this current investigation: 177.8 x 19.1 mm (7 x 3/4 in.) strips which result in a uniaxial stress state and 177.8 x 177.8 mm (7 x 7 in.) which results in a biaxial stress state. Punch rates were chosen based on test system constraints. The 2.12 mm/sec rate caused failure in less than 30 seconds, the 0.212 mm/sec rate in about four minutes and the 0.042 mm/sec rate in about 25 minutes. Table I shows the test matrix for this investigation.

Strain in the sheet was determined by the circle-grid technique [12,13]. A grid, consisting of a repeated

TABLE I - Summary of Punch Rate-Lubrication Combinations Used With Two Samples Widths, 19.1 mm and 177.8 mm

Lubricant	Punch rate mm/sec (in/min)							
	0.042 (0.1)		0.212 (0.5)		0.423 (1.0)		2.12 (5.0)	
Oil	19.1	--	19.1	177.8	19.1	177.8	19.1	177.8
PTFE	19.1	--	19.1	177.8	19.1	177.8	19.1	177.8
RTV	--	--	--	177.8	--	177.8	--	177.8

array of four 2.54 mm (0.1 in) circles in a 6.35 mm (0.25 in) square, was applied electrochemically to the steel surface before testing. Circle dimensions were measured with an image analysis system on a light microscope. All strain measurements were on samples deformed to peak height. The measurements started at the ligament region, the section of sheet between the punch and the die platens and proceeded along the length of the specimen over the pole position, coincident with the travel axis of the punch, to the ligament region on the other edge of the specimen. These data were plotted as strain distributions, i.e. strain as a function of original linear position along the specimen length. The pole position is at point zero and all the failures are plotted in the 'positive' ligament region. Strains determined at each point were the maximum principal strain, oriented along the radial or meridional direction, and the minor principal strain, oriented along the circumferential direction.

The extent of $\gamma \rightarrow \alpha'$ transformation was determined at each strain point with a Forster portable ferrite meter. The Forster number (%M), is a relative measure of the percent volume fraction of the ferromagnetic martensite phase. The volume of material at the head of the meter probe that influences the reading was on the order of the circle size. Prior to deformation, the steel had a Forster number of 0.15%. Again these data are plotted as transformation distributions; Forster No. versus original linear position, and the failures are plotted in the 'positive' ligament region.

Temperature change in the sheet during deformation was determined with type K thermocouple leads spot welded to the specimen in three locations along the specimen length. The first at the pole position (pole), the second at a position 25.4 mm from the first (mid-radius), and the third 50.8 mm from the first (ligament).

RESULTS

19.1 MM WIDE SAMPLES - Strain distributions along the specimen lengths for 19.1 mm wide specimens stretched at a punch rate of 0.423 mm/sec are shown in Figure 2 for samples lubricated with oil and PTFE. The radial strain distribution obtained with oil lubrication exhibits a steady increase on a traverse from pole to ligament. The strain values decrease at the furthest ligament positions due to constraint effects of the die platens. In contrast, the specimens tested with PTFE lubrication showed a relatively constant radial strain value across the punch region with a minor increase in the ligament section. Failure resulted from necking and fracture in the ligament section in both instances. The distributions are symmetrical about the pole position except for the necking which occurred only in one (plotted as 'positive') ligament region. The distributions for both lubrication conditions shown in Figure 2 are typical of specimens tested at all punch rates with the respective lubricant.

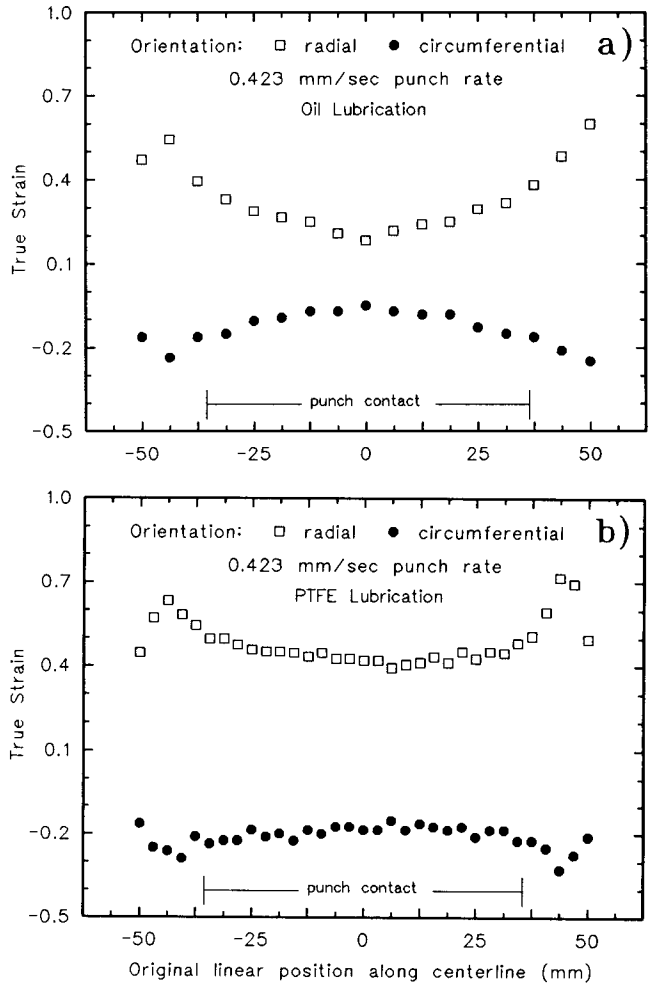

Figure 2. Strain distribution along centerline of 19.1 mm wide, Type 304 stainless steel specimens punch-stretched to failure at 0.423 mm/sec with a) oil lubrication and b) PTFE lubrication.

Table II lists radial strain values at the pole and ligament positions for the four punch rates and two lubrication conditions under review. Uniform strain values are compared because strains associated with necking and fracture are high and depend on the actual circle-grid location. With the oil lubricant, radial strain at the pole position remained essentially constant for all punch rates. However in the ligament region, a slight increase in strain, from 0.48 at 2.12 mm/sec to 0.61 at 0.042 mm/sec, was observed with decreasing punch rate. With the PTFE lubricant, the strain levels at both positions moderately increased with decreasing punch rate, except that the ligament strain values for the specimens tested at a rate of 0.423 mm/sec are higher than those for the specimens tested at a rate of 0.212 mm/sec. This observation is related to the martensite transformation discussed later.

The martensite volume fraction distributions along the specimen lengths are shown in Figure 3 for the 19.1 mm specimen tested with both oil and PTFE lubrication at four different punch rates. As seen in Figure 3a for the oil lubricated specimens, the degree of

TABLE II - Strain Values and Corresponding Forster Numbers from the Uniform Strain Region of 19.1mm Wide Specimens

Punch Rate (mm/sec)	Position	OIL		PTFE	
		ϵ_{radial}	%M	ϵ_{radial}	%M
0.042	Pole	0.22	0.8	0.48	6.5
	Ligament	0.61	14.0	0.60	15.0
0.212	Pole	0.22	0.8	0.39	4.5
	Ligament	0.56	14.0	0.43	6.0
0.423	Pole	0.22	0.50	0.41	5.5
	Ligament	0.54	6.0	0.61	14.0
2.12	Pole	0.22	0.35	0.31	2.0
	Ligament	0.48	1.6	0.40	2.1

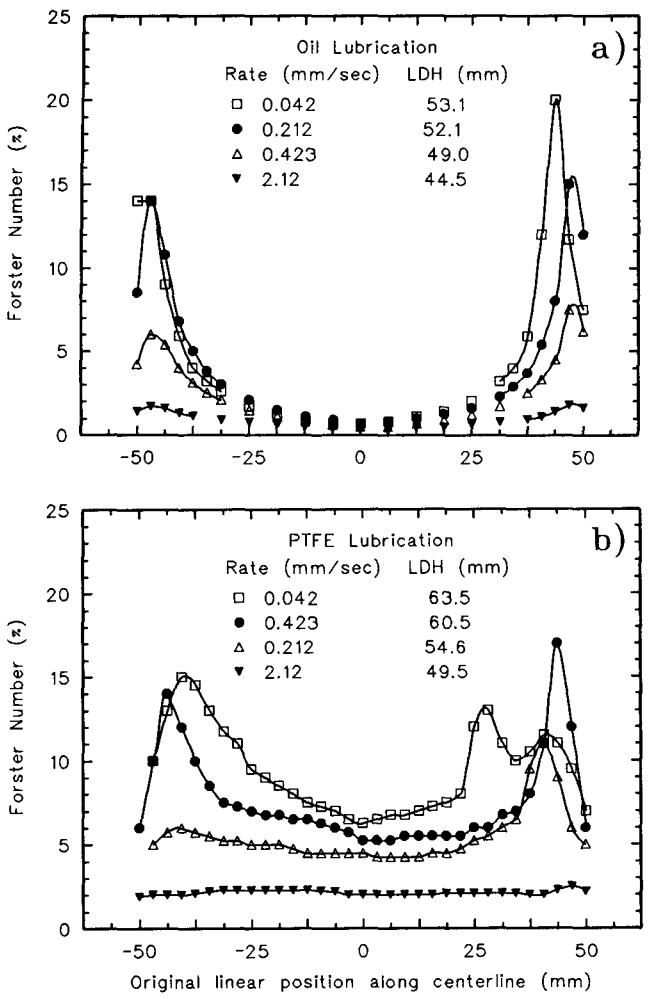

Figure 3. Transformation distribution along centerline of 19.1 mm wide, Type 304 stainless steel specimens punch-stretched to failure with a) oil lubrication and b) PTFE lubrication.

martensite formation is constant for all punch rates at the pole position, but increased with decreasing punch rate in the ligament region. The decrease in Forster No. at the extent of the strain measurements within the ligament is also due to die platen constraint. The higher martensite volume fractions in the ligament regions correspond directly to higher total punch heights at failure. For the PTFE lubricated specimens shown in Figure 3b, the martensite volume fractions, measured at both the pole and ligament positions, increased with a decrease in punch rate. However, as was also shown for the strain profile data, the ranking is reversed for the 0.423 mm/sec and the 0.212 mm/sec data. As with the oil lubricated samples, the LDH values for the PTFE lubricated samples increase with an increase in the volume fraction of strain-induced martensite. Further, at each punch rate, the LDH values for the PTFE lubricated samples are higher than for the oil lubricated samples. The higher LDH values for PTFE samples correspond directly to the higher overall average volume fraction of martensite which forms with strain in the PTFE lubricated samples .

177.8 MM WIDE SAMPLES - Figure 4 shows strain distributions along the specimen length for oil, PTFE and RTV lubrication of 177.8 mm wide specimens stretched at a punch rate of 0.423 mm/sec. The distributions are typical for specimens tested at all punch rates with the respective lubricant. The strain distributions for the 177.8 mm wide specimens tested with oil lubrication show a steady increase in the radial strain from pole to ligament. Die platen constraint causes the strain to drop off at the furthest ligament position. The strain distribution is similar to that observed for the specimens tested with PTFE lubricant except over the center portion of the punch region where the strain values are more uniform. Tests with the RTV

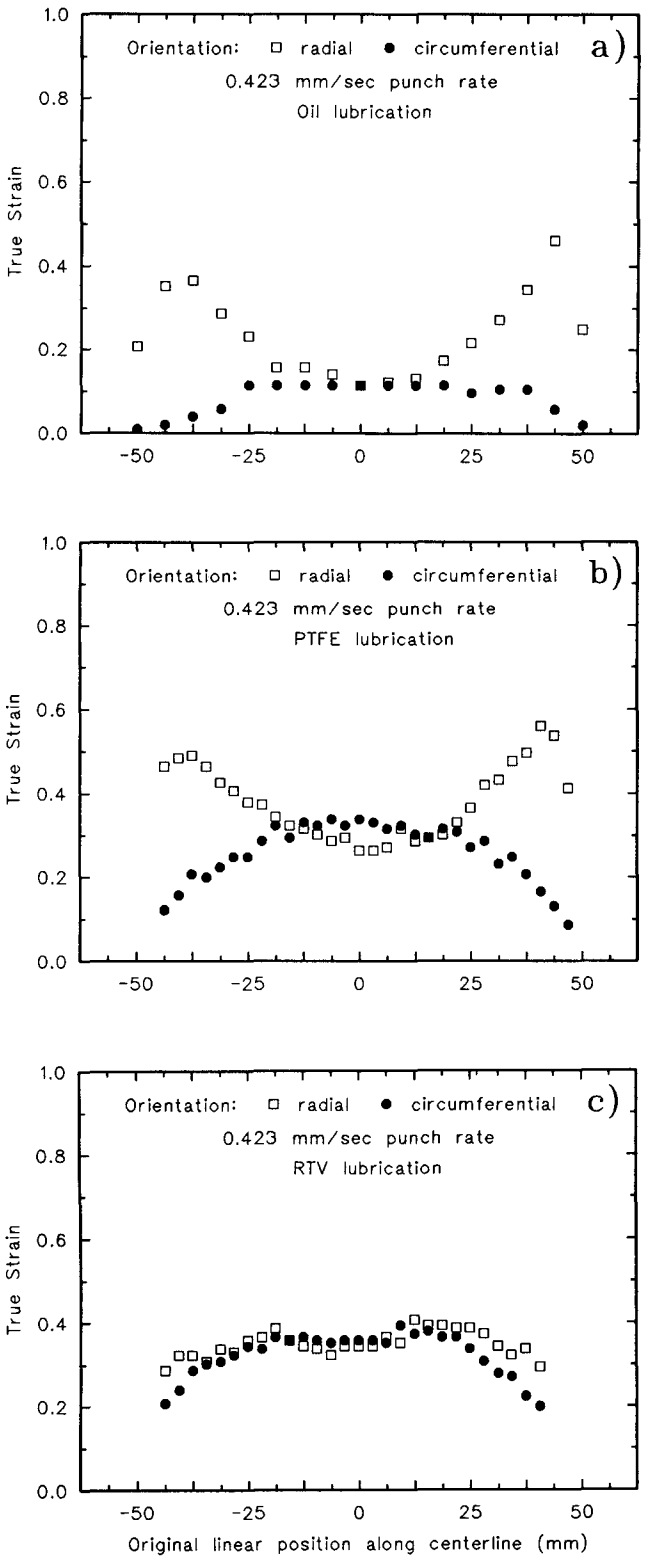

Figure 4. Strain distribution along centerline of 177.8 mm wide, Type 304 stainless steel specimens punch-stretched to failure at 0.423 mm/sec with a) oil lubrication b) PTFE lubrication and c) RTV lubrication.

resulted in uniform strain values across a majority of the punch region with a gradual decrease of strain in the ligament region.

The strain distributions directly reflect the effects of lubrication on the interfacial friction. While the oil or PTFE simply affect how the sheet slides over the punch face, the RTV affects specimen deformation by changing the interfacial friction and the dome geometry. The most striking difference between the lubrication conditions summarized in Figure 4 is in the ligament region where the oil and PTFE lubricated specimens show a significant divergence of the radial and circumferential strains. Failure occurred in the ligament region for oil and PTFE lubricated specimens. The RTV lubricated specimens show only a minor divergence of the two strains in the ligament region. Further, failure in RTV lubricated specimens occurred closer to the pole than in the other specimens.

One important implication of this lubrication effect on strain is related to the construction of the FLC. PTFE lubricated specimen limit strains would plot nearer the plane-strain region of the forming limit diagram (FLD). RTV lubricated specimen limit strains would plot nearer the balanced biaxial stretch region but at a lower principal strain indicating that the FLC falls off in the stretching region of the FLD.

The second implication of the effect of lubrication on strain relates to the accumulation of strain and the corresponding strain and transformation distributions. For the oil or PTFE lubricated specimens, strain is incrementally accumulated over the face of the punch out into the ligament region while for the RTV lubricated specimens, strain is preferentially accumulated in the sheet near the pole of the punch.

Table III lists strain values at the pole and at a location in the ligament directly adjacent to the zone of localized necking and fracture for the three punch rates and lubrication conditions. The strain at the pole position increases as the effective lubrication increases (oil to PTFE to RTV). Similarly the strain at the ligament position is higher for specimens tested with PTFE lubrication compared to oil lubrication. Strains are not affected by punch rate for specimens lubricated with oil. For PTFE and RTV lubricated specimens, strain values decrease as punch rates increase.

The principal strains for uniaxial and biaxial stress states are different. They can however be compared if transformed into equivalent strains with the von Mises effective plastic strain expression. For the uniaxial condition this is equivalent to the maximum principal strain. For the biaxial condition, the effective plastic strain value, ϵ_{eff}, is determined with the following relation [14]:

$$\epsilon_{eff} = \frac{\sqrt{2}}{3}[(\epsilon_1-\epsilon_2)^2 + (\epsilon_1-\epsilon_3)^2 + (\epsilon_2-\epsilon_3)^2]^{1/2} \qquad (1)$$

where ϵ_1, ϵ_2, and ϵ_3, are principal strains. Effective strain distributions along the specimens length are shown in Figure 5 for the 177.8 mm wide specimens tested at three

TABLE III - Strain Values from the Uniform Strain Regions of 177.8 mm Wide Specimens

Punch Rate mm/sec	Position	Oil		PTFE		RTV	
		ϵ_{rad}	ϵ_{cir}	ϵ_{rad}	ϵ_{cir}	ϵ_{rad}	ϵ_{cir}
0.212	Pole	0.13	0.13	0.29	0.34	0.31	0.32
	Ligament	0.36	0.02	0.47	0.20	0.39	0.28
0.423	Pole	0.11	0.11	0.26	0.31	0.33	0.34
	Ligament	0.36	0.02	0.49	0.19	0.34	0.30
2.12	Pole	0.11	0.11	0.22	0.28	0.27	0.27
	Ligament	0.30	0.02	0.48	0.15	0.27	0.19

punch rates with three different lubrications. The distributions show that strain values increase significantly form pole to ligament for the specimens tested with oil. For specimens tested with PTFE, the corresponding strains only slightly increase. The strain values are constant over the pole region for the RTV lubricated specimens and decrease in the ligament region. The distributions obtained with RTV lubrication overlap on one side due to the presence of wide necks which developed prior to failure. Generally higher effective strain values correspond to a lower imposed punch rates and higher LDH values for all lubrication conditions. PTFE and RTV lubricants result in similar strain levels over the center of the punch; the strain values are nearly double those resulting from oil lubrication.

Martensite volume fraction distributions along the specimen lengths are shown in Figure 6 for the 177.8 mm specimens tested at three punch rates with the three lubricants. A clearer distinction between punch rates is shown by the Forster number distributions as opposed to the effective strain distributions. Higher martensite volume fractions are associated with lower punch rates over the entire specimen length with PTFE or RTV lubrication while they are higher only in the ligament region of oil lubricated specimens. Further, higher martensite volume fractions are directly related to higher LDH values.

TEMPERATURE MEASUREMENTS - Peak temperatures for the punch-stretched specimens at failure were found to vary with punch rate and lubrication as shown in Table IV. The temperature increases are primarily due to adiabatic specimen heating with strain. Sliding friction, lubricant heating, and heat of the martensite transformation were assumed to make negligible contribution to the temperature changes. Adiabatic specimen heating is a function of strain rate. As a consequence of geometrical considerations in the hemispherical dome test [11], the effective strain rate increases along the punch face from the pole towards the ligament region and increases in the ligament region with punch displacement. It is therefore expected that adiabatic specimen heating will be amplified by higher punch rates.

Table IV shows that the peak temperature increase in the ligament region of 19.1 mm wide specimens tested with either oil or PTFE lubricant was at least 40°C higher for the faster punch rate. Temperature increases of 40°C or greater have been reported for tensile testing of sheet material [10,11]. A mild temperature increase in the pole region was only seen for the PTFE lubricated 19.1 mm wide specimens tested at the 2.12 mm/sec punch rate.

Table IV also shows that the temperature increased with strain at both pole and ligament positions in the 177.8 mm wide specimens at high and low punch rates for all three lubricants. The temperature increased more in the ligament than at the pole for oil and PTFE lubrication and was higher at the highest displacement rate. In contrast, pole region temperatures were greater than ligament region temperatures with RTV lubrication.

The effects of lubrication on temperature at different locations on the specimen are shown in Figures 7 and 8. Temperature data as a function of time are plotted for thermocouples located at the pole, mid-radius and ligament positions. The time axis directly relates to punch displacement and therefore specimen strain and strain rate. During deformation of the 19.1 mm wide specimens at 2.12 mm/sec punch rate, Figure 7, the mid-radius temperature follows the ligament temperature until contact with the punch and then cools to the pole temperature. Pole and mid-radius temperatures are constant for the oil lubricated specimens but rise with time for the PTFE lubricated specimens due to the increase in strain accumulation over the punch face. Similar profiles occurred at the 0.212 mm/sec punch rate.

Temperature-time profiles for deformation of 177.8 mm wide specimens (Figures 8a and 8b) are similar to the 19.1 mm wide specimens for the oil and PTFE lubrication, except for lower peak temperature values. In contrast to oil and PTFE lubrication, RTV lubrication caused significant pole and mid-radius temperature increases, and only a minor ligament temperature increase (Figure 8c).

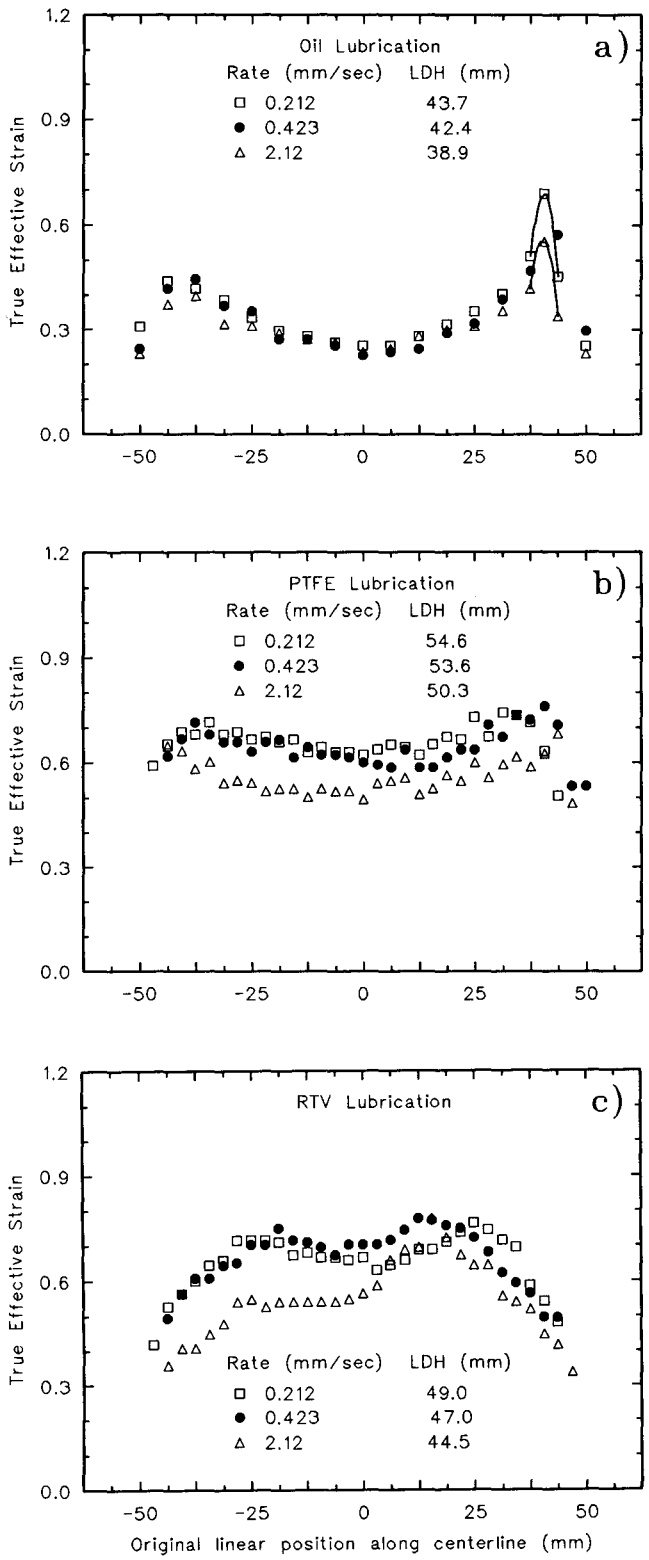

Figure 5. Effective strain distribution along centerline of 177.8 mm wide, Type 304 stainless steel specimens punch-stretched to failure with a) oil lubrication b) PTFE lubrication and c) RTV lubrication.

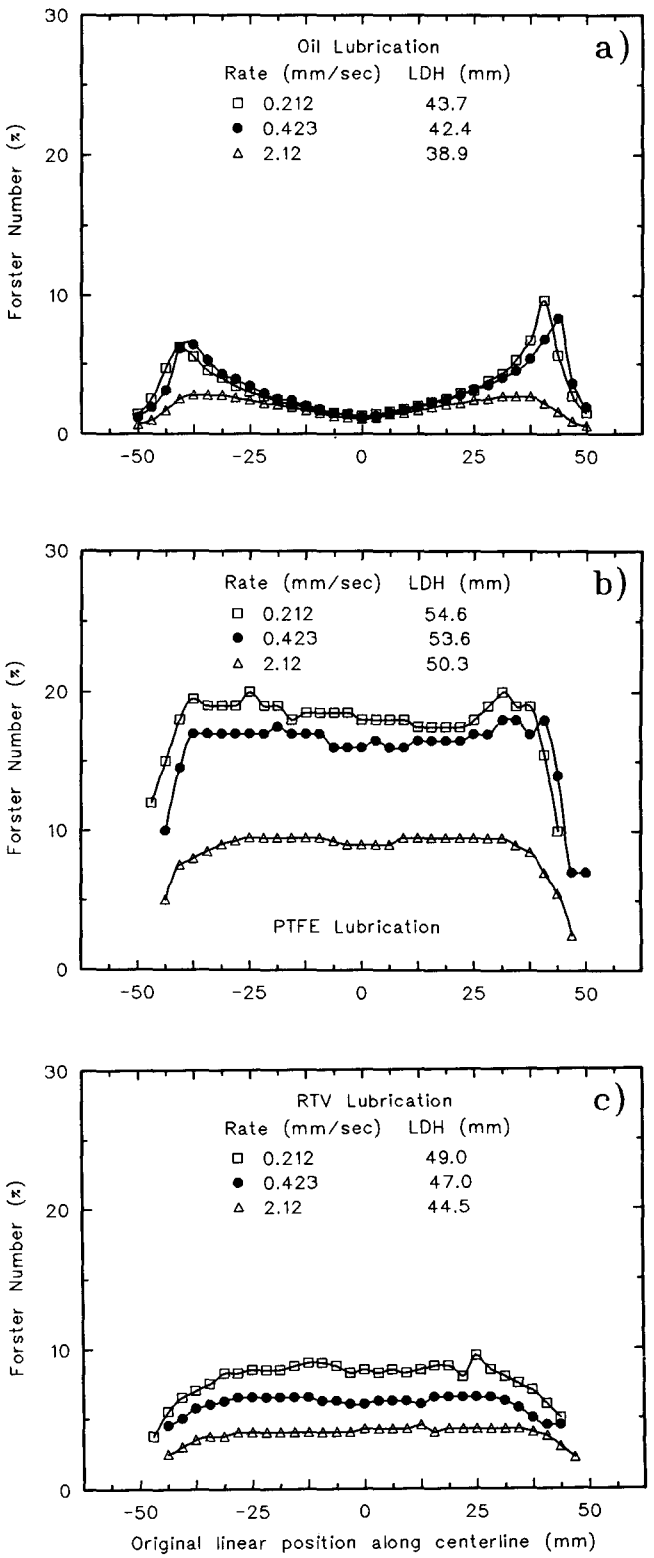

Figure 6. Transformation distribution along centerline of 177.8 mm wide, Type 304 stainless steel specimens punch-stretched to failure with a) oil lubrication b) PTFE lubrication and c) RTV lubrication.

TABLE IV Peak temperatures as a function of punch rate and lubrication at two positions on the 19.1 mm and 177.8 mm wide specimens.

Peak Temperature (°C): 19.1 mm wide specimen					
Lubricant:		oil		PTFE	
Position:		pole	ligament	pole	ligament
Punch Rate: (mm/sec)	2.12	25	88	31	87
	0.212	28	46	27	45

Peak Temperature (°C): 177.8 mm wide specimen							
Lubricant:		oil		PTFE		RTV	
Position:		pole	lig	pole	lig	pole	lig
Punch Rate: (mm/sec)	2.12	31	53	41	85	91	40
	0.212	30	34	32	31	56	30

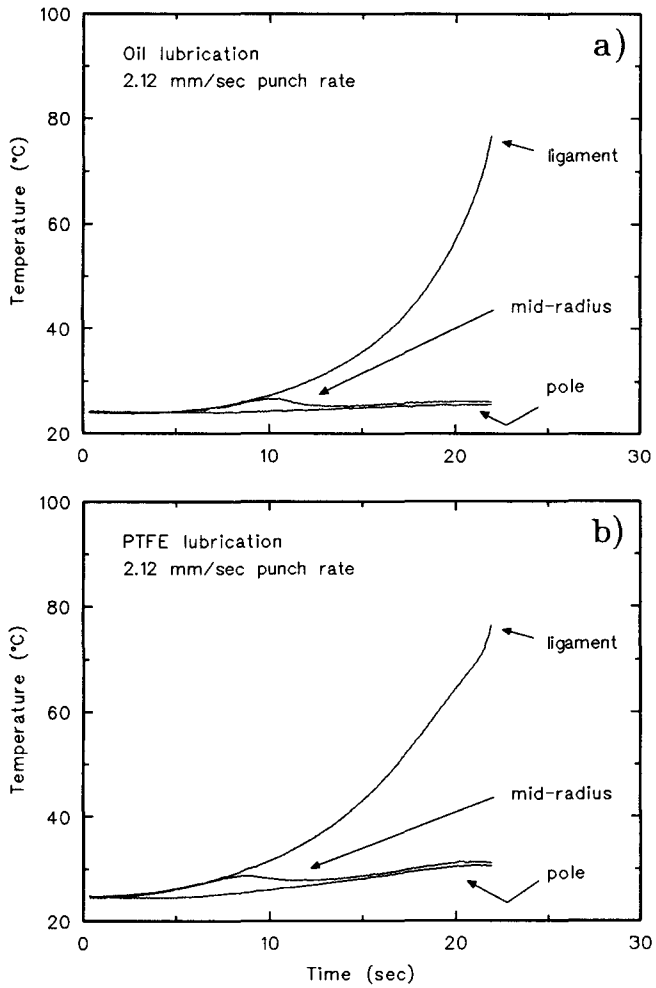

Figure 7. Temperature-time profiles along centerline of 19.1 mm wide, Type 304 stainless steel specimens punch-stretched to failure at 2.12 mm/sec with a) oil lubrication and b) PTFE lubrication.

DISCUSSION

At a given temperature between M_d and M_s, the martensite start temperature, strain-induced martensite transformation is a sigmoidal function of strain as was shown in Figure 1. With increasing strain, the rate of increase in the martensite volume fraction decreases until a maximum (saturation) level is reached. This transformation saturation level both decreases and shifts to higher strains as the deformation temperature increases. This complex interaction of strain and temperature on the martensite transformation and the subsequent influence on formability are discussed by first considering the conditions where low temperature changes have little effect on the martensite transformation and then at conditions where temperature increases significantly affect the martensite transformation.

As shown in Figures 2 and 4 for the 19.1 mm and 177.8 mm wide samples respectively, the strain distribution during stretch forming of 304 stainless steel depends directly on the lubrication condition of the sheet-punch interface. The large variation in radial strain from the pole to the ligament position for the oil lubricated specimens reflects directly the interfacial friction conditions. With punch displacement, as each point on the sheet contacts the punch, the interfacial friction constrains further deformation so that each successive point accumulates incrementally more strain than the previous point. For the PTFE lubricated 19.1 mm wide specimens (Figure 2b), the interfacial friction is significantly lower and thus with punch displacement each point already in contact with the punch continues to deform and accumulate strain resulting in a more constant strain distribution. For the PTFE lubricated 177.8 mm wide specimen (Figure 4b), the radial strain is not constant but increases into the ligament region.

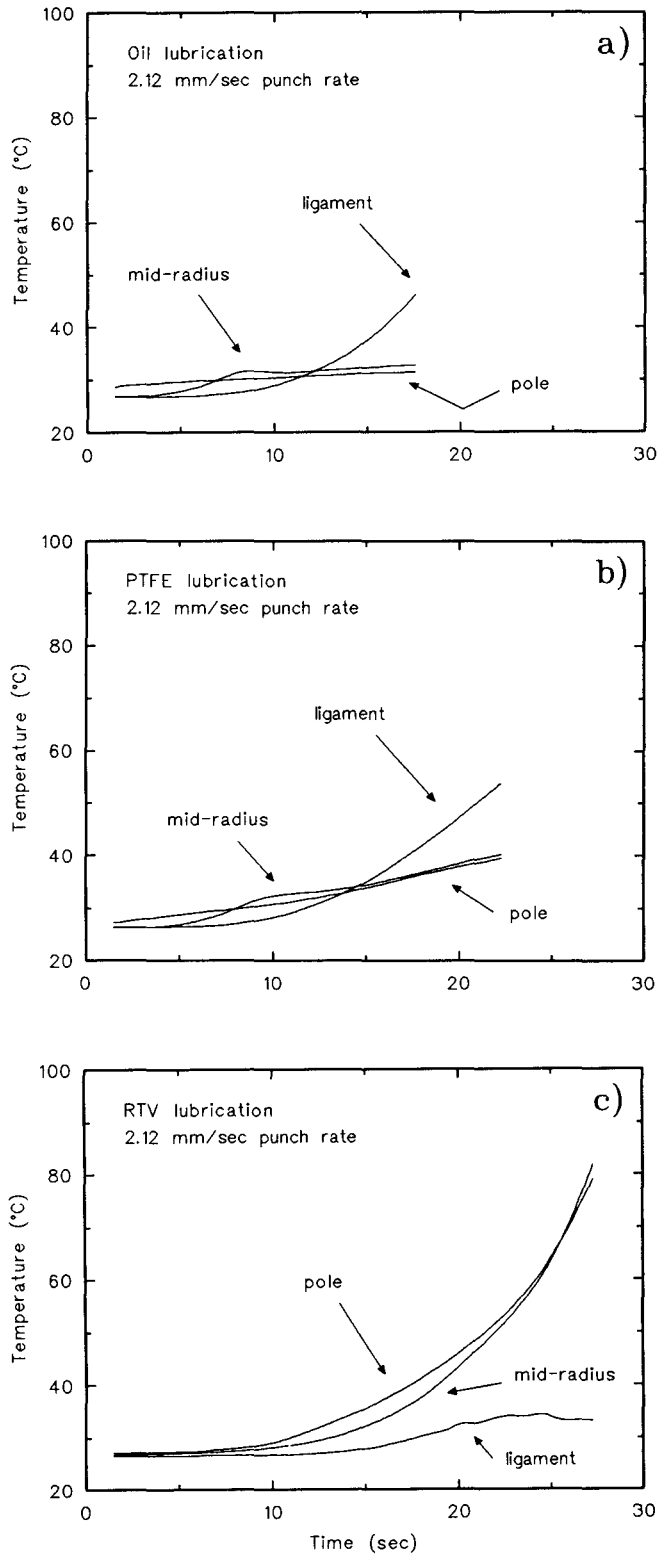

Figure 8. Temperature-time profiles along centerline of 177.8 mm wide, Type 304 stainless steel specimens punch-stretched to failure at 2.12 mm/sec with a) oil lubrication b) PTFE lubrication and c) RTV lubrication.

Using the effective plastic strain to account for the biaxial constraint of the wider specimens results in a constant strain distribution for the PTFE lubricated 177.8 mm wide specimens (Figure 5b). The strain distribution shown by the RTV lubricated 177.8 mm wide specimens (Figure 5c) reflects both the effects of a change in interfacial friction and a geometry change due to the thick rubber layer at the sheet-punch interface. The rubber disk was compressed between the sheet and the punch producing a dome with an effective diameter greater than 101.6 mm thus causing strain accumulations in the pole region without significant strain accumulations in the ligament.

The transformation distributions obtained at the lower punch rates for the oil and PTFE lubricated 19.1 mm wide specimens, Figure 3, and the oil lubricated 177.8 mm wide specimens, Figure 6a, are a result of the effects of interfacial friction on strain distribution as deformation heating was negligible (as shown in Table IV). Correspondingly, the variation in volume fraction of martensite with position mirrors the strain distribution. The increased strain over the pole of PTFE lubricated specimens results in a higher martensite volume fraction (Figure 3b). Increasing lubrication results in an increase in strain distributed over the entire specimen length which also results in an increased volume fraction of martensite over the entire length of the sample.

This relation between strain and volume fraction of martensite is not observed for the PTFE lubricated or RTV lubricated 177.8 mm wide specimens at any punch rate (Figures 6b and 6c). Further, although the strains obtained with RTV lubrication are of a similar magnitude as those obtained with PTFE lubrication (Figures 5b,5c), the associated volume fractions of martensite produced in the RTV lubricated specimens are only one-half those produced in the PTFE lubricated specimens (Figures 6b,6c).

As was shown in Figures 7 and 8, temperature increases occurred at different locations along the sample length based upon the lubrication used. For the 19.1 mm wide specimens, an increased punch rate resulted in a temperature increase in the ligament region for both oil and PTFE lubricated specimens (Figure 7). This temperature rise suppressed martensite formation, and thus lower martensite volume fractions were found in the ligament regions of oil and PTFE lubricated, 19.1 mm wide specimens (Figure 3) and oil lubricated 177.8 mm wide specimens (Figure 6a) deformed at higher punch rates. As a consequence of this temperature increase, lower martensite volume fractions were also found in the pole region of the PTFE lubricated, 19.1 mm wide specimens deformed at higher punch rates (Figure 3b).

The temperature increases shown in Figure 8b for PTFE lubricated 177.8 mm wide specimens are sufficient to cause transformation saturation at the strain levels achieved with this lubricant (Figure 5b). The strain in the ligament region (Figure 5b) coupled with the temperature in the ligament region (Figure 8b) results in the same volume fraction of transformed martensite as does the coupling of the strain in the pole

region (Figure 5b) with the temperature in the pole region (Figure 8b). This saturation results in the constant transformation distribution seen in Figure 6b.

The temperature rise in the pole region of the RTV lubricated specimens is much higher than the temperature rise caused by the other lubricants due to the deformation being concentrated nearer the pole region of these specimens. The temperature-time profiles for the RTV lubricated 177.8 mm wide specimens, Figure 8c, show the significant increases in temperature that occur at the pole and mid-radius positions. Significant depression of the martensite transformation results, even at large strains, leading to the low transformation distributions seen in Figure 6c. Hecker et al. [10] proposed that the decrease on the biaxial stretching side of the forming limit curve for type 304 stainless steel was due to a drop in the work hardening rate because the $\gamma \rightarrow \alpha'$ transformation is lower. In this investigation, the level of martensite transformation in a specimen whose strain values would plot on the biaxial side of the FLD was indeed lowered.

An increase in formability, as measured by the LDH value, is related to the amount of deformation accumulated in the hemispherical dome specimens. For oil lubricated specimens, improved deformation is due solely to the increased stretching which occurs in the ligament region. With improved lubricity, the increased stretching occurs over the punch face as well as in the ligament region. Figures 3 and 6 show the LDH value along with the resulting transformation distribution. A direct one to one relation can be seen between the magnitude of the LDH value and the overall average volume fraction of martensite produced in the specimen. Increased transformation to martensite is accomplished by deformation at temperatures below M_d. The primary requirement for high elongation resulting in greater formability is continued martensite transformation during deformation. Factors promoting transformation are: 1) increased lubrication which allows strain accumulation over the entire specimen, 2) a slower punch rate resulting in a lower strain rate thereby producing less adiabatic specimen heating, and 3) reduced specimen temperature which would result in high transformation saturation values at a given strain. The optimum transformation giving the highest formability would occur at that combination of strain rate and temperature that causes martensite formation to occur at the maximum uniform strain value thereby stabilizing neck formation in the sheet.

The results of this study have several implications with respect to current developments in sheet steel microstructures and forming methodologies. For example, recent analyses of the tensile deformation behavior of a new class of high strength sheet steels with controlled volume fractions of retained austenite showed that ductility is maximized at temperatures where the majority of the deformation induced transformation of austenite to martensite occurs within the neck [15, 16]. Correspondingly, it is anticipated that these high strength sheet steels will exhibit the same dependence on strain rate, temperature, and lubrication as was observed for the type 304 stainless steel of this study. Furthermore, currently consideration is being given to new dry lubricants which will not provide the same effective sample cooling provided by water base lubricants. It is anticipated that the actual sheet temperatures may differ from those currently observed. Thus if the sheet metal undergoes temperature dependent deformation induced transformation, then the degree of transformation and hence extent of formability will depend on the lubricant. Therefore, future sheet steel developments must consider the combined effects of strain and temperature in order to maximize formability.

CONCLUSIONS

The combined effects of lubrication, imposed deformation rate, and deformation heating on the stretch formability of type 304 stainless steel sheet has been evaluated with the punch stretch test. Measured strain distributions directly reflect the constraint effects due to friction at the sheet/tool interface and the combined effects of deformation induced transformation on austenite to martensite and strain induced adiabatic heating. Several specific conclusions were drawn from this study:

- With increased lubricity, more uniform strain distributions developed.
- The observed strain gradients between the punch and the ligament regions of the deformed sheets increased with a decrease in punch rate and mirrored the volume fractions of deformation induced martensite formation at the low displacement rates where negligible deformation heating was observed.
- At high deformation rates where significant adiabatic heating was observed in the ligament sections of the oil and PTFE lubricated specimens and throughout the sample for the RTV lubricated specimens, saturation of the martensite transformation occurs and the observed punch heights at failure were lower than those observed at the lower displacement rates.
- Formability is maximized for those test conditions which promote continued transformation during deformation. The deformation induced austenite to martensite transformation provides and increment of strengthening to stabilize plastic flow and suppress necking.

ACKNOWLEDGEMENTS

The authors acknowledge the support of the Advanced Steel Processing and Products Research Center, an NSF Industry-University Cooperative research center at the Colorado School of Mines.

REFERENCES

1. S.S. Hecker, "Simple Technique for determining Forming Limit Curves", Sheet Metal Industries, vol 52, no 11, 1975, pp. 671-676

2. S.P. Keeler and W.A. Backofen, "Plastic Instability and Fracture in Sheets Stretched over Rigid Punches", Trans ASM, vol 56, 1963, pp. 25-48.

3. R. Heyer and J. Newby, "Effects of Mechanical Properties of Biaxial Stretchability of Low Carbon Steels", Trans. SAE, Paper-680094, vol 77, 1968.

4. S.S. Hecker, "Experimental Studies of Sheet Stretchability", Formability: Analysis, Modeling and Experimentation,ed. S.S. Hecker, A.K. Ghosh and H.L. Gegel, TMS-AIME, Warrendale, PA, 1978, pp.150-182.

5. T.J. Angel, "Formation of Martensite in Austenitic Stainless Steels; Effects of Deformation, Temperature and Composition", J. Iron Steel Inst., vol 177, 1954, pp. 165-174.

6. G.R. Powell, E.R. Marshall, and W.A. Backofen, "Strain Hardening of Austenitic Stainless Steel", Trans ASM, vol 50, 1958, pp. 478-497.

7. G.B. Olson and M. Cohen, "A Mechanism for Strain-Induced Nucleation of Martensitic Transformations", J. Less-Common Metals, vol 28, 1972, pp. 107-118.

8. G.L. Huang, D.K. Matlock, G. Krauss, "Martensite Formation, Strain Rate Sensitivity, and Deformation Behavior of Type 304 Stainless Steel Sheet", Met Trans A, vol 20A, 1989, pp. 1239-1246.

9. G.B. Olson and M. Cohen, "Kinetics of Strain Induced Martensitic Nucleation", Met Trans A, vol 6A, 1975, pp. 791-795.

10. S.S. Hecker, M.G. Stout, K.P. Staudhammer, and J.L. Smith, "Effects of Strain State and Strain Rate on Deformation-Induced Transformation in 304 Stainless Steel: Part 1. Magnetic Measurements and Mechanical Behavior.", Met Trans A, vol 13A, 1982, pp.619-626.

11. D.A. Burford, Frictional and Geometric Effects in Punch-Stretch Sheet Metal Formability Testing", Phd Thesis and SRC Research Report No. MT-SRC-087-042, Colorado School of Mines, Golden, CO, November, 1987.

12. S.P. Keeler, "Circular Grid System - A Valuable Aid for Evaluating Sheet-Metal Formability", Sheet Metal Industries, vol 45, no 497, 1968, pp. 633-641.

13. R.A. Ayers, "Aids for Evaluating Sheet Metal Formability: The Limiting Dome Height (LDH) Test and the Grid Circle Analyzer", Novel Techniques in Metal Deformation Testing, ed. R.H. Wagoner, TMS-AIME, Warrendale, PA, 1983, pp.47-63.

14. Dieter G.E., Mechanical Metallurgy, 2nd Edition, McGraw Hill, New York, 1976, p.90.

15. Yasuharu Sakuma, D.K. Matlock, and G. Krauss, "Intercritically Annealed and Isothermally Transformed 0.15 pct C Steels Containing 1.2 pct Si-1.5 pct Mn and 4 pct Ni: Part I. Transformation, Microstructure, and Room Temperature Mechanical Properties," Metallurgical Transactions A, vol. 23A, 1992, pp. 1221-1232.

16. Yasuharu Sakuma, D.K. Matlock, and G. Krauss, "Intercritically Annealed and Isothermally Transformed 0.15 pct C Steels Containing 1.2 pct Si-1.5 pct Mn and 4 pct Ni: Part II. Effect of Testing Temperature on Stress-Strain Behavior and Deformation-Induced Austenite Transformation," Metallurgical Transactions A, vol. 23A, 1992, pp. 1233-1241.